COUPLED BUNCH INSTABILITY AND ITS CURE AT J-PARC RCS

Y. Shobuda*, P. K. Saha, H. Hotchi, H. Harada, T. Takayanagi, F. Tamura, N. Tani, T. Togashi, T. Toyama, Y. Watanabe, K. Yamamoto, M. Yamamoto, J-PARC Center, Ibaraki, Japan
Y. H. Chin, Y. Irie, KEK, Tsukuba, Japan

Abstract

The RCS at J-PARC is a kicker-impedance dominant machine, which violates the impedance budget from a classical viewpoint. Nevertheless, we have recently succeeded to accelerate a 1-MW equivalent beam by making maximum use of the space charge effect on the beam instabilities. In this report, we explain the manipulation to suppress the beam instability, at first. Then, we discuss some issues to suppress the beam instabilities for beams with much smaller transverse emittance, as well as the present status of our efforts to reduce the kicker impedance toward the realization of the higher beam power at the RCS.

INTRODUCTION

The 3-GeV RCS at J-PARC [1], which is a kicker-impedance dominated machine [2], aims to achieve a megawatt-class beam. Two bunched beams ($N_b = 4.15 \times 10^{13}$ particles per bunch) are accelerated from 400 MeV (Lorentz-$\beta \simeq 0.713$) to 3 GeV (Lorentz-$\beta \simeq 0.971$) during 20 ms with the repetition rate of 25 Hz. Eight kickers are installed into the RCS. A schematic picture of the present kicker magnet is shown in the left panel of Fig.1. The real part of the horizontal impedance $Z_T(\omega)$ for one kicker is shown in the right panel of Fig.1. The impedance is roughly proportional to the Lorentz-β [3].

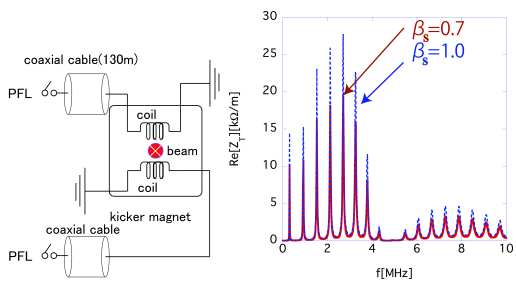

Figure 1: A schematic picture of the present setup of the kicker magnet (left) and the kicker-impedance $Z_T(\omega)$ (right).

Though the conventional Sacherer's formula [4] without space charge effects estimated the beam growth rate by using the kicker impedance as an input parameter, such estimation differs significantly from the measured results at the RCS, especially at the low energy [2].

Recently, we have developed a new theory that includes coupled-bunch mode μ and head-tail mode m of instabilities with space charge effects [2]. Based on this theory, we have demonstrated a 1-MW equivalent beam with larger transverse emittance by suppressing the beam instabilities [2].

* yoshihiro.shobuda@j-parc.jp

In the next section, let us explain the manipulations to suppress beam instabilities at the RCS

MANIPULATIONS TO SUPPRESS BEAM INSTABILITIES AT THE RCS

The beam growth rate is given by the real part of $j\omega_0\nu$ by solving the following dispersion relation for ν as a function of nominal betatron tune Q_x [2]:

$$1 \simeq -\sum_{p=-\infty}^{\infty} \frac{je^2 N_b M \pi \beta_s^2 \langle\beta_x(s)\rangle}{8\pi^3 J_{x0} p_s R \left(m\frac{d\nu_L}{dJ_x} + \frac{d\nu_x}{dJ_x}\right)} \left[1+ \frac{(\nu - m\nu_{L0} - \nu_{X0}) e^{-\frac{(\nu - m\nu_{L0} - \nu_{X0})}{\left(m\frac{d\nu_L}{dJ_x} + \frac{d\nu_x}{dJ_x}\right) J_{x0}}} \Gamma\left[0, -\frac{(\nu - m\nu_{L0} - \nu_{X0})}{\left(m\frac{d\nu_L}{dJ_x} + \frac{d\nu_x}{dJ_x}\right) J_{x0}}\right]}{\left(m\frac{d\nu_L}{dJ_x} + \frac{d\nu_x}{dJ_x}\right) J_{x0}}\right]$$
$$\times \left| J_m \left[\left(\nu + \mu + pM - \frac{Q_x \xi_x}{\eta}\right)\sqrt{\frac{2\omega_0 J_{L0}|\eta|}{c p_s \beta_s \nu_{s0}}}\right]\right|^2$$
$$\times Z_T\left(\omega_0(\Re[\nu] + \mu + pM)\right), \quad (1)$$

where

$$J_{x0} = \frac{\beta_s E_s \epsilon_{x,rms}}{c}, \quad (2)$$

$$\nu_{L0} = \nu_{s0} + \left.\frac{dY'_{coh,0}(J_L)}{dJ_L}\right|_{J_L = J_{L0}}, \quad (3)$$

$$\nu_{X0} = Q_x + \frac{\langle\beta_x(s)\rangle}{p_s} Y'_{coh,2}(J_{L0}), \quad (4)$$

$$m\frac{d\nu_L}{dJ_x} + \frac{d\nu_x}{dJ_x} \simeq m \left.\frac{dY'_{coh,2}(J_L)}{dJ_L}\right|_{J_L = J_{L0}} \frac{\langle\beta_x(s)\rangle}{p_s} + 3\left\langle\beta_x^2(s)\right\rangle Y'_{coh,4}(J_{L0}), \quad (5)$$

$$\sigma_x = \sqrt{\langle\beta_x(s)\rangle \epsilon_{x,rms} + \langle D^2(s)\rangle \left(\frac{\Delta p}{p}\right)^2}, \quad (6)$$

$$\sigma_z = \frac{c}{\omega_0}\sqrt{\frac{2J_{L0}|\eta|\omega_0}{E_s \nu_{s0}}}, \quad (7)$$

ω_0 is angular revolution frequency; h is harmonic number, a is chamber radius; c is light velocity; $E_s = cp_s/\beta_s$; p_s is the longitudinal momentum of the synchronous particle; β_s and γ_s are the Lorentz-β and the Lorentz-γ of the particle; η is slippage factor; ξQ_x is chromaticity in the horizontal direction; Z_0 is impedance of free space; $J_n(x)$ is the Bessel function; $\Gamma[0, z]$ is the incomplete Γ-function; M is the number of bunches (buckets); $\epsilon_{x,rms}$ is the root mean square

(rms) emittance of the beam; J_{L0} is the longitudinal beam emittance; ν_{s0} and Q_x are the nominal synchrotron and the horizontal tunes; ν_{L0} and ν_{X0} are the coherent synchrotron and the betatron tunes; $\beta_x(s)$ is the Twiss parameter; $D(s)$ is the dispersion function; R is the average radius of the RCS; and $\langle \cdots \rangle$ denotes the average value around the ring. The functions $Y'_{coh,0}(J_L)$, $Y'_{coh,2}(J_L)$ and $Y'_{coh,4}(J_L)$ are derived in the reference [2]. The bunching factor B_f is defined as the average current divided by the peak current.

The second terms of Eqs.(3) and (4) show the coherent synchrotron and the betatron tune shifts, respectively. Equation (5) shows the non-linear effect on the synchrotron and betatron oscillations of the beam centroid due to the space charge effects.

Figure 2 shows the theoretical results of B_f- (left), $\epsilon_{x,rms}$- (middle), and ξQ_x- (right) dependences of the beam growth rate for 1-MW equivalent beam. In the left and middle panels, ξQ_x is fully corrected only at the injection energy by a DC power supply. In the left and right panels, we assume $\epsilon_{x,rms} \simeq 100/6\beta_s\gamma_s$ mm.mrad.

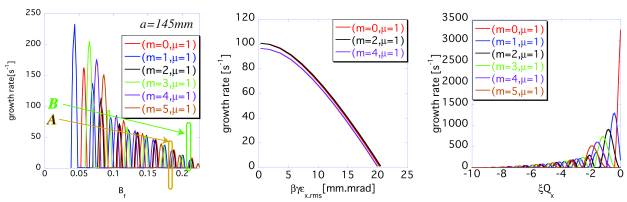

Figure 2: Theoretical results of B_f- (left), $\epsilon_{x,rms}$- (middle), and ξQ_x- (right) dependences of the beam growth rate for 1-MW beam at 15 ms for $Q_x = 6.45$ and $a = 145$ mm.

As the left panel of Fig.2 shows, the beam growth rate can be theoretically suppressed by adjusting B_f, owing to the beam stabilized regions on B_f (for example, around the areas A and B), created by the space charge effects. Contrary to the conventional understanding, the suppression of beam growth rate is possible by compressing the bunch length, as well. The beam growth rate for different modes (m, μ) follows the different characteristic comb-like structures along B_f, which originates from the head-tail motion of the beam. For an ultra-relativistic beam, the beam growth rates excited by the different modes (m, μ) are sufficiently overlapped along B_f. That is why, there is no beam stabilization region on B_f. On the other hand, for not so ultra-relativistic beams like at the RCS, the space charge damping effect significantly reduces the beam growth rate. Consequently, the beam stabilized regions emerge along B_f at the RCS.

The existence of the area A was already demonstrated at the RCS [2]. The beam growth rate is quite sensitive to the indirect space charge effects stemming from the chamber wall. It is expected that the smaller chamber radius a is preferable to suppress the beam instabilities [2].

In order to activate the space charge damping effect, coming from the longitudinal charge distribution of the beam, it is essential that the beam has a finite transverse beam size. Mathematically, the non-linear effects on the oscillations diminish for the infinitesimal pencil beams. As shown in the middle panel of Fig.2, the beam instability can be suppressed by enlarging the transverse beam emittance $\epsilon_{x,rms}$.

The right panel of Fig.2 illustrates ξQ_x-dependence of the beam growth rate. Following the conventional understanding, the beam growth rate can be suppressed by increasing $|\xi Q_x|$ in the negative direction at the RCS, owing to the Landau damping effect.

These theoretical comprehensions basically provide the explanation why we can accomplish 1-MW beam for larger transverse emittance beam, though the RCS violates the impedance budget from a classical point of view.

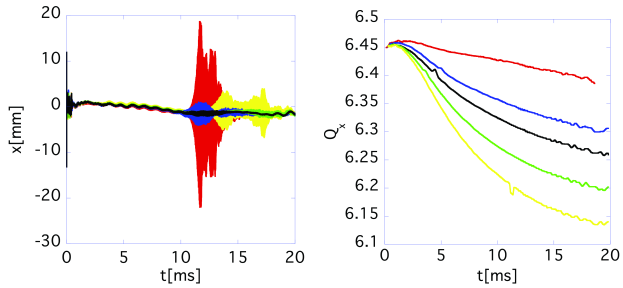

Figure 3: The measured beam positions (left) for five different tune tracking patterns shown in the right panel for 1MW-beam with 100 π-painting injection scheme [5], where ξQ_x is fully corrected at the injection energy by a DC-power supply. The chromaticity approaches the natural chromaticity ($\xi Q_x = -10.3$) as the beam energy is increased.

The left panel of Fig.3 shows the measured beam positions for five different tune tracking patterns shown in the right panel with the same color for 1MW-beam. The beam instability occurs at the latter part of the acceleration period. This can be understood as follows. The beam has a larger transverse beam size at the lower energy, where the space charge damping effect can be easily activated. As the beam energy becomes higher, the space charge damping effect becomes more deactivated, which excites the beam instability. While the chromaticity correction is weakened at the high energy, the effect is insufficient to suppress the beam instability. Thus, the beam instability occurs at the high energy.

The contribution from the kicker impedance to the beam growth rate depends on Q_x through $J_n(x)$ in Eq.(1). The summation of p over $Z_T(\omega)$ and $J_n(x)$ expresses the wakes caused by the previous passages of beams through the kickers. As the right panel of Fig.1 shows, the kicker impedance has the spike structure, which produces the tune dependence of the beam growth rate. Thus, the beam growth rate can be minimized by optimizing Q_x, corresponding to the black line in the right panel of Fig.3. Finally, as the black line of the left panel of Fig.3 illustrates, the beam instability is suppressed by choosing this tune tracking pattern.

In the next section, let us discuss some issues to suppress the beam instabilities for beams with smaller transverse emittance by comparing the theoretical with the measured results.

ISBN 978-3-95450-182-3

HOW TO SUPPRESS THE BEAM GROWTH RATE FOR SMALLER TRANSVERSE EMITTANCE BEAMS

In the following measured results, unless specified otherwise, we consider a beam made with 50 π injection scheme, where the tune tracking is chosen as the red line in the right panel of Fig.3, generating the highest beam growth rate.

The left panel of Fig.4 shows the measured result of $\epsilon_{x,rms}$-dependence of beam growth rate. The measured data demonstrates that the beam can be stabilized as $\epsilon_{x,rms}$ is enlarged. The middle panel suggests that the existence of the beam stabilization area B for $Q_x = 6.45$ in the left panel of Fig.2 by suppressing the beam growth rate with the slight reduction of B_f. Fast decrease in B_f around 13 ms of the black line in the right panel is caused by the rigorous beam instability shown by the black line in the middle panel.

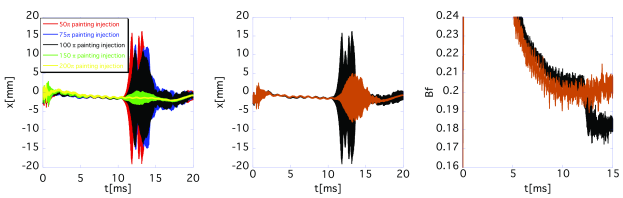

Figure 4: Measurement results of $\epsilon_{x,rms}$- (left) and B_f- (middle) dependences of the beam growth rate of 910-kW beam. The right panel shows the corresponding measured B_f with the same color (black and brown) as with in the middle panel.

Figure 5 shows the measured ξQ_x-dependence of beam growth rate. Presently, the 830-kW beam can be stabilized, regardless of the choice of tune tracking pattern, by intentionally increasing $|\xi Q_x|$ in the negative direction by 15 % compared to the natural chromaticity, which is limited by the present power of sextupole magnets. In order to accomplish the higher beam power, or 1-MW beam power with much smaller transverse beam size, it is vital to reduce the kicker impedance itself.

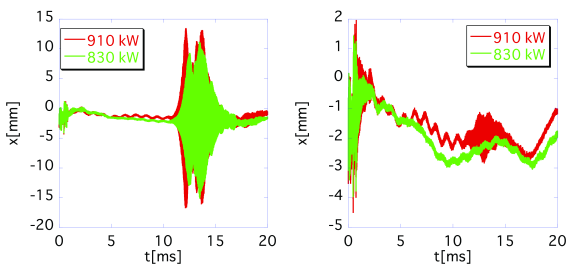

Figure 5: Measured beam positions for different ξQ_x patterns. In the left panel, ξQ_x is 60 % corrected at the injection energy by a DC power supply, while in the right panel, ξQ_x is increased by 15 % compared to the natural chromaticity after 10 ms by activating sextupole magnets.

One candidate of the reduction scheme is shown in the left panel of Fig.6, where the kicker cables are terminated by resistors with diodes. The diodes isolate the resistors from PFL. Since the diodes are non-linear devices, $Z_T(\omega)$ depends on the beam power. The measured result for 750-kW beam is shown in the right panel of Fig.6. Comparing it with the right panel of Fig.3, $Z_T(\omega)$ is remarkably reduced. Figure 7 shows the theoretical result of beam growth rates for $\epsilon_{rms} \simeq 40/6\beta_s\gamma_s$ mm.mrad (left) and for $\epsilon_{rms} \simeq 50/6\beta_s\gamma_s$ mm.mrad (right), where ξQ_x is fully corrected only at the injection energy by a DC power supply. The reduction scheme is a promising candidate to accomplish 1-MW beam or more with $\epsilon_{rms} \gtrsim 50/6\beta_s\gamma_s$ mm.mrad, regardless of the choice of Q_x.

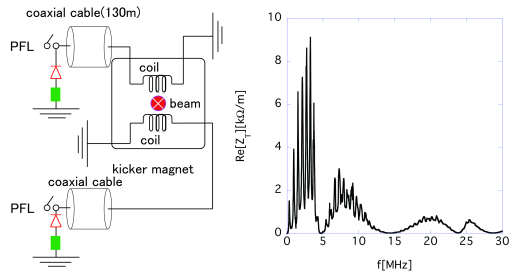

Figure 6: A schematic picture of the setup of the kicker magnet (left) and the effective measured horizontal kicker-impedance $Z_T(\omega)$ for 750-kW beam (right).

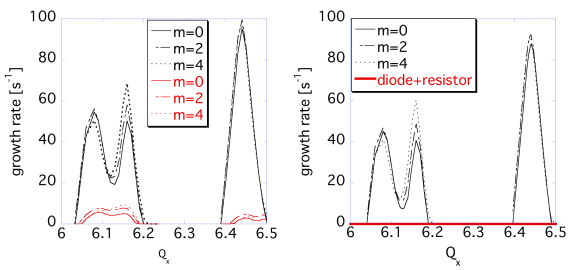

Figure 7: Dependence of the theoretical result of the beam growth rate at 15 ms on Q_x. The red and black lines show the results for the kicker of Fig.3 and for the kicker of Fig.6.

SUMMARY

In a low energy proton machine, such as the RCS, the violation of the impedance budget from a classical viewpoint, which does not take the space charge force into account, is not vital to achieve high intensity beams, except the beams with smaller transverse beam size. They can be realized by optimizing the machine's (beam) parameters, i.e. the bunching factor, transverse emittance, tune, chromaticity, and so on.

For beams with smaller transverse emittance, the intentional increase of chromaticity by the activation of sextupole magnets, or the reduction of the kicker impedance is an effective way to suppress the beam instability.

REFERENCES

[1] J-PARC, http://j-parc.jp/index-e.html

[2] Y. Shobuda et al., "Theoretical elucidation of space charge effects on the coupled-bunch instability at the 3 GeV rapid cycling synchrotron at the Japan Proton Accelerator Research Complex", Prog. of Theor. and Exp. Phys., vol. 1, p. 013G01, Jan. 2017, https://doi.org/10.1093/ptep/ptw169

[3] Y. Shobuda et al., "Measurement scheme of kicker impedances via beam-induced voltages of coaxial cables", Nucl. Instr. Meth. A, vol. 713, pp. 52-70, 2013.

[4] F. Sacherer, "Theoretical aspects of the behaviour of beams in accelerators and storage rings", in 1st International School of Particle Accelerators "Ettore Majorana", p. 175, 1977.

[5] P. K. Saha et al., "Direct observation of the phase space footprint of a painting injection in the Rapid Cycling Synchrotron at the Japan Proton Accelerator Research Complex", Phys. Rev. ST:AB, vol. 12, p. 040403, 2009.